/

LA-UR -83-2269

LA-UR--83-2269

DE83 015927

Los Alamos National Laboratory is operated by the University of California for the United States Department of Energy under contract W-7405-ENG-36

Conf-830719--20

TITLE THE VELOCITY OF SOUND BEHIND STRONG SHOCK WAVES IN 2024 Al

AUTHOR(S) R. G. McQueen, J. N. Frit . E. Morris

SUBMITTED TO American Physical Society Topical Meeting on Shock Waves in Condensed Matter, Santa Fe, NM, July 18-21, 1983.

DISCLAIMER

Los Alamos
Los Alamos National Laboratory
Los Alamos, New Mexico 87545

FORM NO 836 R4
ST NO 2629 5/81

MASTER

THE VELOCITY OF SOUND BEHIND STRONG SHOCK WAVES IN 2024 Al*

R. G. McQueen, J. N. Fritz and C. E. Morris

Los Alamos National Laboratory
Los Alamos, New Mexico 87545

Rarefaction waves were produced by impacting a target with a thin plate. An optical technique was used to determine where the rarefaction from the back surface of the impactor overtook the shock wave induced in a step wedge target. Bromoform was placed on the front surface. When the shock reached the liquid it radiated steadily until the rarefaction from the impactor overtakes it. The times when this occurred were used to determine where the rarefaction just overtook the shock in the target, and thus the sound velocity. The leading edge of this rarefaction wave travels at longitudinal sound velocity in solids. This velocity increases smoothly with pressure until shock heating causes the material to melt. The data indicate that melting on the Hugoniot of 2024 Al begins at about 125 GPa and is completed at 150 GPa.

INTRODUCTION

Probably one of the most important measurements that can be made on shocked materials, after its basic Hugoniot has been measured, is to determine the velocity of sound at pressure. There has been a continuing effort to do this for many years with the first success reported by Al'tshuler et al. (1) in 1971. In most experiments the velocity of sound is determined by measuring when or where the rarefaction wave from the back surface of an impactor overtakes the shock-wave in a target plate. The VISAR (2) and ASM probe (3) experiments allow variation of that basic geometry by observing the reflections in the target through transparent windows or insulators. The experiments described here are of the shock-wave rarefaction overtake type using optical detectors to determine where the overtake occurs.(4) 2024 Al was chosen for this work because it has been used as a standard for determining the equation-of-state for many materials. A better knowledge of the yield strength and Grüneisen parameter, $V(dP/dE)_V$, could be of considerable importance.

A thin plate was accelerated by explosive products which impacted a target plate several times thicker. A shock wave propagates through the target and back through the impactor. The rarefaction velocity to be determined originates at the HE-driver interface, and it propagates through the driver and the target plate eventually overtaking the shock wave causing it to decay with further run. The rarefaction wave before interacting with the shock front has been described by Courant and Friedrich (5) as a simple wave whose states can be determined by rays called characteristic emanating from the HE-driver interface. A schematic of the system is shown in Fig. 1. Here U_s is the shock velocity and C^L the Lagrangian sound velocity, which is related to the sound velocity, C, by the relation

$$C = C^L (\rho_o/\rho) \qquad (1)$$

Ignoring the dashed lines it can be seen from the figure that the intersection of C^L and U_s in the target gives the location of the overtake position. If R is the ratio of target to driver thickness where this occurs then

$$C^L = U_s(R+1)/(R-1) = U_s R^* \qquad (2)$$

In order to reach higher pressures than are possible with symmetrical impacts, we used iron impactors for the experiments above 100 GPa. For an unsymmetrical impact experiment the equation for calculating R^* becomes

$$1/R^*_T = 1-U_T/RU_D(1+1/R^*_D) \qquad (3)$$

Here the U's are shock velocities in the target, T, and driver, D. R again is the actual target to driver thickness ratio.

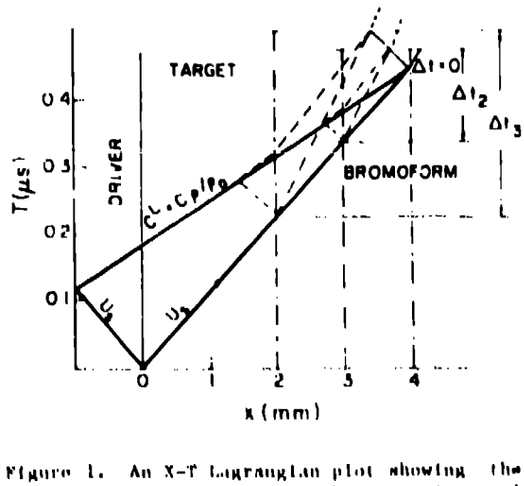

Figure 1. An X-T Lagrangian plot showing the load characteristics and the time interval measured at each target thickness.

* Work supported by the US DOE.

It was mentioned that the location of the catch up was determined by optical analyzers. These are indicated in the figure. It can be seen that when the shocks and rarefactions pass these interfaces that the flow is modified as indicated by the dashed lines. However the lead characteristic is still linear and the plot of the Δt's (these are the length of time the shock runs unperturbed through the analyzer) as a function of their position must also be linear and the extrapolation to $\Delta t = 0$ gives the location in the target where catch up occurs. The Δt's for any level are determined independently from the others. In principle two levels could suffice for this measurement, but usually five or so levels are used, and on a few occasions as many as ten have been used. Some oscilloscope records obtained on a high pressure experiment are reproduced in Fig. 2. A plot of Δt vs target thickness is given in Fig. 3. This is a very high quality experiment. The results are usually not this good.

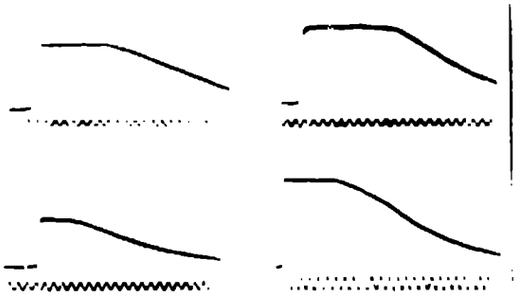

Figure 2. Reproduction of four records obtained on a high pressure shot

For the analyzers we use materials that radiate like a black body when subjected to strong shock waves. The halogen carbons and hydrocarbons seem to possess this property, as well as quartz and some glasses. We have used bromoform, $CHBr_3$, in these experiments because of its high, 2.89 kg/l, density, convenience and radiative properties. The target assemblies usually consisted of a pair of step wedges each with five different thickness levels. The wedges were enclosed in a Plexiglas box which was filled with Bromoform at the firing site. The center of each step on the wedge was viewed through a small aperture ~1 mm in diameter, and a pair of baffles ~2 mm in diameter, with a 0.6 mm diameter quartz fiber located ~20 mm from the aperture. The light pipes were mounted on the face of 931 type photomultipliers (PM), which were connected directly to Tektronix 454 or 485 oscilloscopes. The voltage divider circuit designed by Beck (6) was used. The recording systems were tested with a spark gap, and were found to have rise times from 1 to 2 ns. Occasionally this type of rise time was observed on the records but 4 to 6 ns seemed to be more typical.

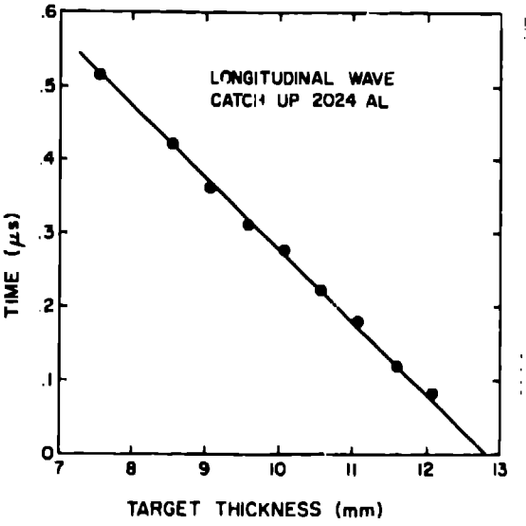

Figure 3. A plot of the target thickness vs. catch up times for one experiment.

RESULTS

We have obtained data from 50 GPa to 150 GPa. One set of records, reproduced in Fig. 2, obtained on a high pressure experiment show one relatively well defined break. The shock pressure in the 2024 Al for this experiment was 147 GPa and was sufficiently high to melt the material. At lower pressure the first wave to overtake the shock front is due to the longitudinal component, which is followed by a bulk rarefaction wave. The longitudinal release usually causes a well defined break in the records as can be seen in Fig. 4. However, there can be seen an additional change in slope when the rarefaction traveling at the bulk sound velocity overtakes the shock front. This feature is not well defined. Our records are also complicated by the fact that the Bromoform causes additional interactions. However a measure of the bulk velocity can be obtained from these records. The results for one experiment are shown in Fig. 5. Some amplification occurs if the longitudinal component of the rarefaction is allowed to decay in the 2024 Al target rather than in the Bromoform.

We have measured the amplitudes of the relative radiation in the unperturbed shock front and where the bulk wave appears. Although somewhat subjective, since many of the records show considerable curvature where this occurs, a reasonably good measure of this was obtained on an experiment designed to observe this feature. We found the ratio of the amplitude of the relative light intensities to be ~1.7:1. From knowledge of the radiation-pressure behavior of Bromoform this implies a decrease

Figure 4. Reproduction of a record on an experiment designed to measure the bulk sound velocity as well as the longitudinal velocity.

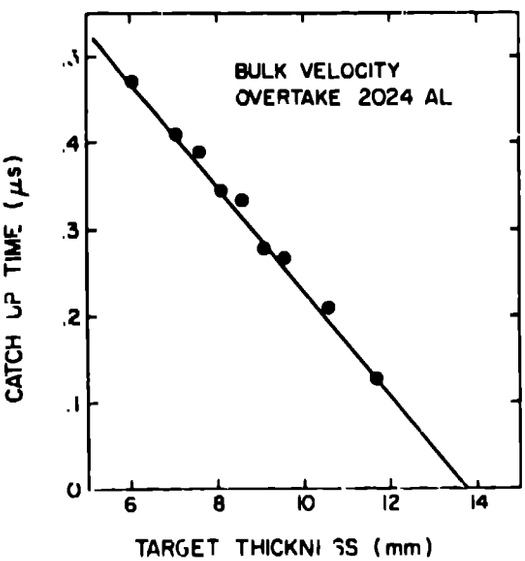

Figure 5. The overtake time vs target thickness for the bulk rarefaction wave.

in pressure from 100 GPa to 95 GPa. This does not mean that the material has a 5 GPa yield strength. If one assumes that the shocked 2024 Al is on the yield surface the deviatoric stress is only ~1.5 GPa. However, when using these data to compute bulk sound velocities and the value of the Grüneisen parameter the pressure should be reduced ~5 GPa, and the required shock velocity reduced accordingly. This has been done for the few experiments designed to determine the bulk sound velocity. The data are summerized in Table I and plotted in Fig. 6.

DISCUSSION

As expected the first wave arrival data yields wave velocities that can be fitted with a smooth curve. Most of the data are within a percent of this curve. However there are points that are further from the curve than

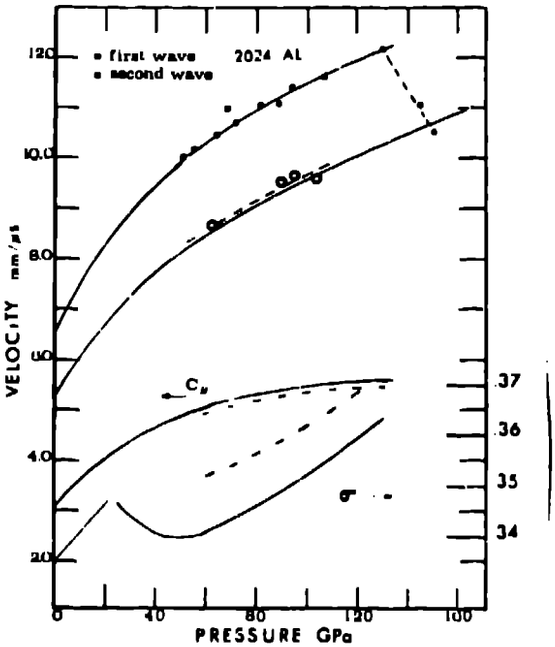

Figure 6. Wave velocities as a function of pressure. The dots and circles are velocities calculated from the experiment data. The shear velocity, Cu, and Poisson's ratio, σ, were calculated from the upper sets of curves.

TABLE I. SOUND VELOCITIES IN 2024 Al

P GPa	U_B mm/μs	C_L mm/μs	C_B mm/μs
52	8.33	10.04	
55	8.44	10.17	
66	8.89	10.47	
68	8.95	11.0	8.7*
71	9.09	10.73	
82	9.46	11.04	
89	9.74	11.1	
94	9.89	11.45	9.6*
100	10.09		9.70*
108	10.34	11.51	9.47*
125	10.85	12.20	
145	11.37	11.03	
150	11.56		10.55

* These velocities have been corrected for the longitudinal decay.

can be explained by simple scatter. We believe this is due to mistakes of unknown origin. Three of the four second wave arrival measurements appear to be slightly higher than the solid curve, which was calculated from the Hugoniot data with $\sigma=\sigma_0\gamma_0$ where $\gamma_0=2.0$.(7) We have drawn a dashed line from between the 125 GPa and 150 GPa data points. We believe this curve puts upper limits on the pressure where melting begins and is completed. It

super heated solid states exist the actual melting pressure would be lower. In addition to our data we have used the data of Asay and Chhabildas (8) to fit the lower end of the upper solid curve. On the basis of the two solid curves we have calculated the shear velocity, C_μ, drawn in the 3 to 5 mm/μs range on the figure. This is concave downward as expected because of shock heating effects. The same two curves were used to calculate Poisson's ratio, σ, which is plotted on the bottom of the graph.

We note that three of the four second wave velocity points lie a substantial amount above the calculated bulk sound velocity curve. Based on those three points and the lower one we have drawn in the dashed curve. This is approximately one percent higher than the calculated curve. We then calculated C_μ and σ again based on the longitudinal velocity curve and the dashed curve. These are also plotted as dashes. Since the two curves are now closer together C_μ decreases and σ increases a bit. It thus appears that the shear wave velocity and Poisson's ratio are probably determined to within a couple of percent.

If the dashed bulk velocity curve is correct, then γ must decrease by about 15% in the 100 GPa pressure regime. If the 150 GPa point in the liquid is used to calculate γ, it is found that γ must increase by about 10%. It must be remembered that this is a single point which should be verified even though it appears to be a very high precision experiment.

We have plotted the P-ρ Hugoniot of 2024 Al in Fig. 7 along with approximate melting phase boundaries. This is an empirical curve where the initial slope was determined from aluminum melting data, and the relative curvature estimated from calculated 2024 Al isentropes. We have tied it to the Hugoniot at 125 and 150 GPa. It can be seen that the indicated change in volume at the melting point is reasonable.

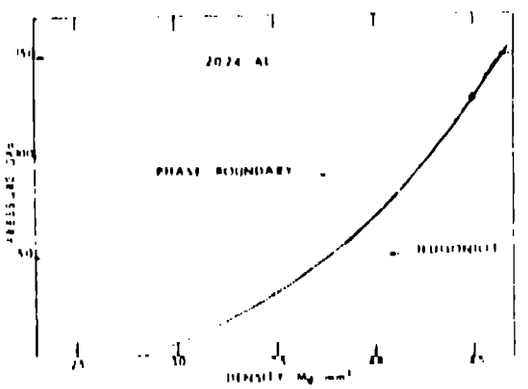

Figure 7. Pressure-density curves for the 2024 Al Hugoniot.

The Lindemann melting criteria predicts that 2024 Al should melt at approximately 100 GPa when using a Grüneisen γ indicated by the experiments. We also note that if the melting phase line followed curves of constant entropy melting would also be predicted to occur at ~100 GPa. Some experimental data were presented by McQueen et. al. (9) to justify this simple concept.

CONCLUSIONS

From these measurements and calculations we conclude that melting on the Hugoniot for 2024 Al begins at ~125 GPa and is completed at ~150 GPa. The longitudinal release wave velocity is quite well determined with the bulk wave velocity less well. We believe the shear moduli and Poisson's ratio are determined to ~2 to 3%. The Grüneisen parameter is probably determined to about 10%. More measurements should be made so that the velocity of the bulk wave can be determined to higher precision in both the solid and liquid phase. The yield strength, which might be important when 2024 Al is used as a standard, also needs to be better determined. The indicated release pressure of 5 GPa for the longitudinal component is just in the range where this type of correction might become needed.

REFERENCES

1. Al'tshuler, L. V, Brazhnik, M. I., and Telegin, G. I. S., Telegin, J. Appl Mech. Tech. Phys. 12 (1972) 921.
2. Barker, L. M., IUTAM Symposium, Paris (Gordon and Breach, New York 1967).
3. Fritz, J. N. and Morgan, J. A., Rev. Sci. Instrum. 44 (1973) 215.
4. McQueen, R. G., Hopson, J. W. and Fritz, J. N., Rev. Sci. Instrum. 53(2) (1982) 245-250.
5. Courant, R. and Friedrichs, K. O., Supersonic Flow and Shock Waves (Interscience Publishers, Inc., New York, 1948) 416.
6. Beck, G., Rev. Sci. Instrum. 47 (1976) 5.
7. McQueen, R. G., Marsh, S. P., Taylor, J. W., Fritz, J. N. and Carter, W. J., High Velocity Impact Phenomena (Academic Press Inc., New York, (1970) 293-417.
8. Asay, J. R., Chhabildas, L. C., Shock Waves and High-Strain Rate Phenomena in Metals (Plenum Press), New York and London (1981) 417-431.
9. McQueen, R. G., Carter, W. J., Fritz, J. N. and Marsh, S. P., Accurate Characterizations of the High-Pressure Environment. (Government Printing Office NBS SP-326) 219-227.